

Bifurcation Analysis and Chaos Detection in Power Systems

S. Grillo, S. Massucco, A. Morini, A. Pitto, F. Silvestro

University of Genova – Intelligent Electric Energy Systems Laboratory

Emails: samuele.grillo@unige.it, stefano.massucco@unige.it, andrea.morini@unige.it,
andrea.pitto@unige.it, federico.silvestro@unige.it

Abstract— Power systems show a complex non-linear behaviour due to different phenomena widespread over different time frames. Thus, power system stability is a significant research issue. Bifurcation theory can contribute to face these power system security problems. The study of local bifurcations and chaos through the analysis of power system equations can provide a deep insight into the complex behaviour of such large and interconnected systems. This paper describes the numerical continuation methodology and it shows an application example to voltage control in power systems.

Index Terms— Bifurcations, chaos, power systems, numerical continuation

I. INTRODUCTION

Power Systems are very large scale interconnected systems which can show rich nonlinear dynamic phenomena both under normal and emergency operating conditions. Their complex dynamic behaviour is due to the fact that the dynamic phenomena are spread over different time frames. These phenomena are roughly divided into three categories: mainly mechanical events (due to f/P control perturbations), mainly electrical events (due to v/Q control perturbations) and electromechanical events (connected to rotor swing problems), as noted in [1]. [2] describes one of the most well-established classifications of stability phenomena in power systems.

The liberalized market environment has caused an increased exploitation of the electrical transmission system (also known as the grid), thus making it work closer and closer to its limits. This fact has increased researchers' interest in voltage stability problems.

Thus, bifurcation theory, which has been already applied to several scientific fields, from the biological field up to the medical one, has been recently applied in [3], [4], [5] also to power system issues such as voltage problems.

This theory investigates the change in the asymptotic behaviour of a nonlinear system as some parameters of the system itself vary.

In-depth studies also revealed the existence of chaotic phenomena inside power systems, i.e. of undeterministic oscillations in a deterministic nonlinear system. A chaotic system is characterized by a very strong sensitiveness with respect to its initial conditions. Researchers, such as the authors of [6], found at least three different routes to chaos also inside very simple power systems.

This paper analyzes the primary voltage control of a

generator on an infinite bus by means of bifurcation theory techniques, thus identifying the influence of some system parameters on the steady-state behaviour of the grid. Moreover it investigates the relationship between the system parameters and the chaotic behaviour of the network.

II. BIFURCATION THEORY FOR POWER SYSTEMS

A. Some hints on theoretical aspects

A power system is modelled in the typical form of a non-linear dynamic system with state x :

$$\dot{x} = f(x, \mu), \quad x \in \mathcal{R}^n, \mu \in \mathcal{R}^p \quad (1)$$

where μ represents the vector of the system parameters that can be varied during the analysis.

In a fixed point (an equilibrium or a steady state condition) $x_0(\mu)$, the stability of system (1) is determined by the eigenvalues of the Jacobian $J = \partial f / \partial x$ evaluated in $x(\mu_0)$.

Bifurcations are defined as “qualitative” changes of the asymptotic behaviour of the system family (1) which is obtained by varying the μ components. In general, two dynamic systems are called qualitatively similar or “equivalent” if they have the same number of equilibria, of limit cycles with the same type of stability and if the relative positions of these invariant sets and the shapes of their regions of attraction are similar, as stated in [7].

In particular, local bifurcations can be identified by observing the Jacobian eigenvalues of the invariants which meet at the bifurcation condition.

This paper considers the following kinds of bifurcation, already described in [7]:

- Saddle-node bifurcations (or *fold* or *Limit Point*);
- Hopf bifurcations;
- Fold bifurcations of Limit Cycles;
- Period Doubling bifurcations;
- Generalized Hopf bifurcations.

The aforementioned bifurcations are briefly described in the following.

A stable and an unstable equilibrium coalesce and disappear at a LP bifurcation, which is characterized by a zero real eigenvalue of the Jacobian matrix $J(x_0, \mu_0)$. Sufficient conditions for a LP bifurcation in system (1) are:

$$f(x_0, \mu_0) = 0, \left. \frac{\partial f}{\partial x} \right|_{(x_0, \mu_0)} = 0, \left. \frac{\partial f}{\partial \mu} \right|_{(x_0, \mu_0)} \neq 0, \quad (2)$$

$$\left. \frac{\partial^2 f}{\partial x^2} \right|_{(x_0, \mu_0)} \neq 0$$

In power systems this bifurcation is typically associated to voltage collapse phenomenon.

The Hopf bifurcation is characterized by a pair of purely imaginary eigenvalues of the Jacobian $J(x_0, \mu_0)$. When a parameter varies, an initially stable equilibrium can become unstable and stable cycles with growing amplitude can originate around this equilibrium. If the cycles generated by this bifurcation are stable the Hopf bifurcation is called "supercritical", while if they are unstable, it is called "subcritical".

The mathematical condition for a Hopf bifurcation is that the Jacobian matrix $J(x_0(\mu), \mu)$ has a pair of complex conjugate eigenvalues $\alpha(\mu) \pm j\beta(\mu)$ and that for a specific value of the parameter $\mu = \mu_0$ the following conditions hold:

$$\alpha(\mu_0) = 0, \quad \beta(\mu_0) > 0$$

$$\text{and } \alpha'_{\mu}(\mu_0) \neq 0 \quad (3)$$

and the residual eigenvalues of $J(\mu_0)$ have non-zero real parts.

For the study of cycle stability it is necessary to define the so called Poincarè map \mathcal{P} together with a proper local reference system ξ on a surface transversal to the cycle [7].

Once defined the Jacobian matrix as $A = \left. \frac{d\mathcal{P}}{d\xi} \right|_{\xi=0}$, the cycle is stable if all the eigenvalues of the Jacobian matrix $(\eta_1, \eta_2, \dots, \eta_{n-1})$ are inside the unitary circle, i.e. if $|\eta_i| < 1 \quad \forall i = 1, \dots, n-1$.

The set $\ell = \{1, \eta_1, \eta_2, \dots, \eta_{n-1}\}$ represents the so-called "Floquet multipliers".

When the family of dynamic systems (1) is analysed, it is important to notice that these multipliers depend on the values of the parameters in vector μ . In particular:

- if the parameter variation makes one real multiplier cross the border of the unitary circle along the real positive semiaxis, i.e. $\eta(\mu_c) = 1$, then a fold bifurcation of limit cycles occurs;
- if the parameter variation makes one real multiplier cross the border of the unitary circle along the real negative semiaxis, i.e. $\eta(\mu_c) = -1$, then a period doubling bifurcation occurs.

In case (a) a stable cycle and an unstable one coalesce and disappear as the bifurcation parameter varies, while in case (b) a stable cycle (period-1 cycle) becomes unstable and a stable double period cycle (period-2 cycle) is produced.

The Generalized Hopf (GH) bifurcation is a codimension 2 bifurcation, i.e. generated by the intersection of two

bifurcation curves related to the same invariant set. In particular, a GH point is given by the intersection of a subcritical and a supercritical Hopf bifurcation curve; also a Limit Point of Cycles (LPC) curve stems from this point.

After the description of bifurcations, some notions on chaos are briefly presented. Chaos is defined as "a long term aperiodic behavior in a deterministic system which shows extreme sensitiveness to the initial conditions", as noted in [8]. In the system under test the so called "Feigenbaum chaos" will be detected. This route to chaos is originated by subsequent period doublings of stable cycles which lead to a chaotic attractor.

In order to decide if an oscillation is chaotic, different indicators can be used. Among them there are the Lyapunov exponents, which measure the separation speed of two infinitely close trajectories.

From a mathematical point of view, the linearization of system (1) leads to the following variational equation:

$$\dot{y} = f_x(x, \mu)y \quad (4)$$

where the Jacobian matrix is evaluated along the specific trajectory $x(t, x_0)$.

For each assigned initial condition $y(0)$ the solution $y(t)$ is given by:

$$y(t) = \Phi(t) \cdot y(0) \quad (5)$$

where matrix $\Phi(t)$, called fundamental solution matrix, is the solution of the associated system:

$$\dot{\Phi} = f_x(x(t, x_0), \mu) \cdot \Phi \quad \Phi(0) = I \quad (6)$$

Now the eigenvalues of matrix $\Phi(t)$ are called $\lambda_i(t)$, $i = 1, \dots, n$. These eigenvalues represent the stretching along the main axes. The Lyapunov exponents are thus defined as:

$$L_k = \lim_{t \rightarrow \infty} \frac{1}{t} \ln(\lambda_k(t)) \quad k = 1, 2, \dots, n \quad (7)$$

This exponent represents the speed of stretching or shrinking in the i -th direction in the state space \mathfrak{R}^n along the solution $x(t, x_0)$. In other words, the trajectory will put away its neighbouring trajectories in a specific direction if the Lyapunov exponent is positive, otherwise it will attract its neighbours in a specific direction.

Some typical examples of Lyapunov exponents applications are discussed (it is assumed that $L_1 \geq L_2 \geq \dots \geq L_n$): in the case of "stable equilibrium" all Lyapunov exponents L_i are negative; in the case of "stable limit cycle" it holds $L_1 = 0$ & $L_k < 0 \quad k = 2, \dots, n$, where the first exponent refers to the direction of the stable cycle; in the case of "strange or chaotic attractor" in 3D, the following conditions hold $L_1 > 0, L_2 = 0, L_3 < 0$ with $L_3 < -L_1$; for a strange attractor in 4D, these conditions hold:

$$L_1 > 0, L_2 = 0, L_4 \leq L_3 < 0 \quad (\rightarrow \text{chaos})$$

$$\text{or } L_1 \geq L_2 > 0, L_3 = 0, L_4 < 0 \quad (\rightarrow \text{iperchaos})$$

B. Numerical Continuation Method: the tool

The mathematical method adopted is the Numerical Continuation Method (NCM). A smooth function $F: \mathfrak{R}^{n+1} \rightarrow \mathfrak{R}^n$ is considered. The aim is to calculate the solution curve of the equation $F(x)=0$. The numerical continuation is a technique useful to calculate a sequel of points which approximate the solutions of $F(x)=0$. Most algorithms, including MATCONT [9], adopt a numerical ‘‘predictor-corrector’’ integration method.

Some smooth scalar functions, called ‘‘test functions’’, which systematically have regular zeros at the singularity points, are defined in order to detect the singularities (i.e., the bifurcation points) on the solution branches.

III. AN APPLICATION EXAMPLE TO VOLTAGE STABILITY IN POWER SYSTEMS

A. System Model and Data

In order to analyze the potentialities of the NCM, a simple electric power system, consisting of a synchronous generator connected to an infinite bus through a purely inductive line, has been examined (see Figure 1). The infinite bus voltage V_{net} is equal to its nominal value (1 p.u.); its phase is used as the angle reference for the system and it is 0.

The generator is modelled as a third order model, with two mechanical state variables (the speed deviation ω and the rotor angle δ) and an electric state variable (the transient emf E'). Moreover, there is an additional state variable E_{fdx} due to the automatic voltage regulator (AVR). The synchronous generator has a proportional voltage regulator with a gain K_A and a delay T_A together with a static wind-up voltage limiter.

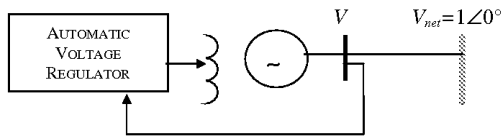


Figure 1. Power system under test

The voltage controller model, already described in [6], is shown in Figure 2, where E_{fdx} represents the ideal field voltage of the controller, $E_{fd real}$ the real field voltage, V_{ref} the voltage setpoint of the AVR, $E_{fd min}$ and $E_{fd max}$ respectively the minimum and maximum threshold of the limiter.

The nonlinearity of the wind-up limiter has been replaced by the following continuous function:

$$E_{fd_real} = 2 \cdot \left(\frac{E_{lim}}{2 \cdot \pi} \right) \cdot \text{actg}(FX) + \frac{E_{lim}}{2} \quad (8)$$

$$\text{with } FX = a \cdot (2 \cdot E_{fdx} - E_{lim}) \cdot e^{b(2 \cdot E_{fdx} - E_{lim})^2}$$

where E_{lim} represents the threshold amplitude of the limiter.

The limiter is asymmetric ($E_{fd min} = 0$ p.u. and $E_{fd max} = 5$ p.u.), because a thyristor semiconrolled rectifier has been considered.

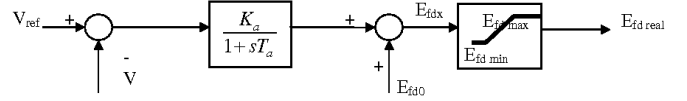


Figure 2. Block diagram of the voltage controller

The dynamic equations describing the system are:

$$\dot{\delta} = \omega_0 \cdot \omega$$

$$\dot{\omega} = \left(-D \cdot \omega + P_T - \frac{E'}{x + x'_d} \sin \delta \right) / M \quad (9)$$

$$\dot{E}' = \left(-\frac{x + x_d}{x + x'_d} E' + \frac{x_d - x'_d}{x + x'_d} \cos \delta + E_{fd real} \right) / T'_{d0}$$

$$\dot{E}_{fdx} = \left(-K_A \cdot (V - V_{ref}) - (E_{fdx} - E_{fd0}) \right) / T_A$$

$$\text{with } E_{fd real} = 2 \cdot \left(\frac{E_{lim}}{2 \cdot \pi} \right) \times \text{actg} \left(a \cdot (2 \cdot E_{fdx} - E_{lim}) \cdot e^{b(2 \cdot E_{fdx} - E_{lim})^2} \right) + \frac{E_{lim}}{2}$$

$$\text{and } V = \frac{1}{x + x'_d} \cdot \sqrt{\left(x'_d + x E' \cos \delta \right)^2 + \left(x E' \sin \delta \right)^2}$$

In the previous x'_d represents the d -axis transient reactance, x_d the d -axis synchronous reactance, x the line series reactance on system base, M the moment of inertia (in seconds) and T'_{d0} the d -axis transient time constant.

The system under test can be written in a formulation which is useful for the use of NCM:

$$\dot{x} = f(x, \mu) \quad x \in \mathfrak{R}^4; \quad \mu \in \mathfrak{R}^4 \quad (10)$$

where $x = [\delta, \omega, E', E_{fdx}]$ and $\mu = [P_T, D, K_A, V_{ref}]$.

The values of the fixed parameters are shown in Table 1.

Table 1. System data

M	x_d	x'_d	x	T_A	T'_{d0}
10 s	1.0 p.u.	0.4 p.u.	0.5 p.u.	1 s	10 s
E_{lim}	a	b	ω_0	E_{fd0}	V_{net}
5 p.u.	0.23	0.1058	377 rad/s	2 p.u.	1.0 p.u.

B. Simulation aims and comments on results

The aims of the simulations are: a) to analyze the system steady state behaviour in case of parameter variations; b) to investigate the effect of the previously defined system parameters (the components of μ vector) on different bifurcations (saddle-node, Hopf, period doublings); c) to identify the effect of the same parameters on the chaotic behaviour coming from subsequent period doublings.

First of all, it is interesting to analyze the power system behaviour for fixed values of D , K_A and V_{ref} ($D=2$, $V_{ref}=1.05$ p.u., $K_A=190$ p.u./p.u.) in case of activated limiter. If the value of parameter P_t is steadily increased the steady state behaviour

of the simple system changes considerably. At first the dynamic response of state variable δ for two different values of P_t , respectively 0.70 p.u. and 0.85 p.u., has been analyzed. In the former case the system steady state behaviour tends to a stable equilibrium, in the latter case it tends to a stable cycle.

In fact, the numerical continuation method identifies an Hopf bifurcation point for $P_t = 0.76$ p.u.. At $P_t=1.047$ p.u. the NCM also finds a period doubling bifurcation. The continuation of the period-2 cycles allows to detect two fold bifurcations of limit cycles; in particular, at $P_t=1.05$ p.u. the stable period-2 cycles coalesce with unstable cycles which in turn coalesce with stable cycles at $P_t=0.95$ p.u.. In this way between $P_t=0.95$ p.u. and $P_t=1.05$ p.u. there are two stable attractors (period-1 and period-2 cycles) separated by an unstable invariant set (unstable period-2 cycle).

Figure 3 shows the steady state system trajectories in the space plane $\delta-\omega$ in case of a small perturbation (Figure 3a) and a significant perturbation (Figure 3b) of the initial condition (with $\mu = [1.0; 2.0; 190; 1.05]$).

In Figure 3a the system trajectory tends to a stable period-1 cycle, on the other hand in Figure 3b it tends to a stable period-2 cycle, which is larger than the period-1 cycle.

These considerations indicate that such a simple power system may show a complex behaviour also for realistic values of its parameters.

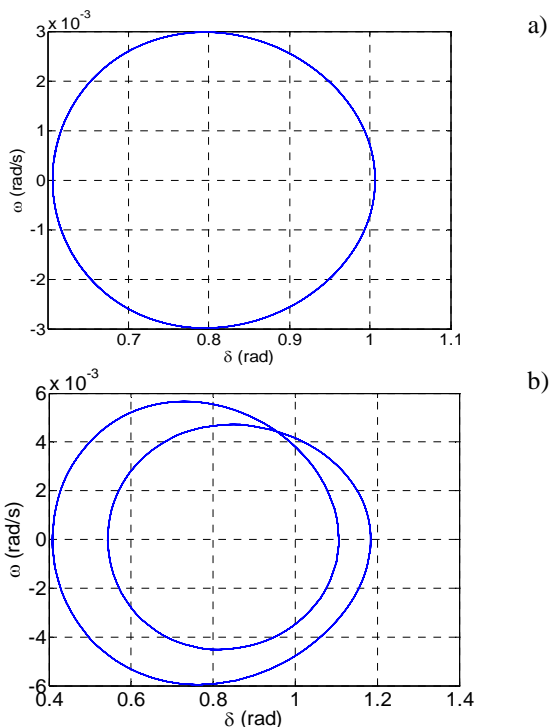


Figure 3. Steady state system trajectories in the space plane $\delta-\omega$ in case of a) small perturbations, b) large perturbations of the initial condition

Figure 4 shows the Hopf bifurcation curve in the bifurcation plane $P_t - D$ both with and without the voltage limiter, using K_A as the curve parameter and assuming $V_{ref}=1.05$ p.u.

The two horizontal lines define the range of realistic values for D , which can reasonably vary from -10 to +20. In Figure 4a it can be noticed that an increase of the AVR gain causes

the Hopf curve to move towards lower P_t values. This fact means that D being unchanged the value of P_t which makes the stable equilibrium undergo a Hopf bifurcation diminishes if the AVR gain increases.

Thus, although a gain increase causes a higher response speed and a higher static precision of the AVR, it can also cause the beginning of a quite complex dynamic for lower values of P_t . In Figure 4b the solid line arrow indicates the movement of the Hopf curve due to the gain increase.

Moreover the dash-dot lines indicate the approaching of the GH points among which there is a supercritical Hopf bifurcation curve.

These points reciprocally approach until they disappear; in fact, for $K_A \geq 190$ almost the whole Hopf bifurcation curve in Figure 4b is characterized by subcritical bifurcations.

Moreover one can observe that the first part of the Hopf curve in Figure 4a (for low values of P_t) is made up of supercritical Hopf bifurcations, while in Figure 4b it is made up of subcritical curves. In Figure 4a there are stable cycles on the right of the Hopf curve (for realistic values of D) and these cycles are the protagonists of cascading period doublings and consequently of the Feigenbaum route to chaos.

On the contrary, the absence of the voltage limiter determines the generation of unstable cycles on the right side of the curve, which prevents this chaos type.

The effect of the parameter V_{ref} on the Hopf bifurcation curves has been investigated. Even if the variation range of this parameter is limited, the effect on the Hopf bifurcation curve is significant. The increase of V_{ref} causes the whole curve to move towards higher values of P_t , D being equal.

Now it is interesting to analyze the effect of parameters V_{ref} and K_A on the fold bifurcation curve.

The dependence of the fold curve on parameter K_A is quite weak both with and without the limiter. In fact even after a wide increment of the gain (from about 50 p.u./p.u. to over 300 p.u./p.u.) one discovers a slight increase of the value of P_t at which the fold bifurcation occurs (it oscillates from 2.02 p.u. to 2.09 p.u.).

After that, the authors analyze the effect of V_{ref} on the value of P_t at which the fold bifurcation occurs. The influence of the voltage setpoint is much more significant than the effect of K_A on the fold curve; in fact in spite of the limited range of the voltage setpoint, the value of P_t at which the fold bifurcation occurs increases by about 10% when V_{ref} is raised.

The influence of the two mentioned parameters on the Period Doubling (PD) curve can be then analyzed (Figure 5).

Figure 5a shows the first PD curve in presence of variations of the two parameters $P_t - K_A$. One can observe that the curve is monotonically decreasing; thus, when the gain increases the value of P_t at which the first PD occurs considerably decreases. In particular, the value of P_t at which the first PD occurs is almost a decreasing linear function of K_A .

In Figure 5b there is a GPD (GPD = Generalized Period Doubling) point in all the three curves; the GPD point occurs at the zero of the c coefficient of the PD normal form, as noted by [9]. Along each of the three curves the GPD point indicates the stability change of the double-period cycle; moreover a fold bifurcation curve for double period cycles stems from this point.

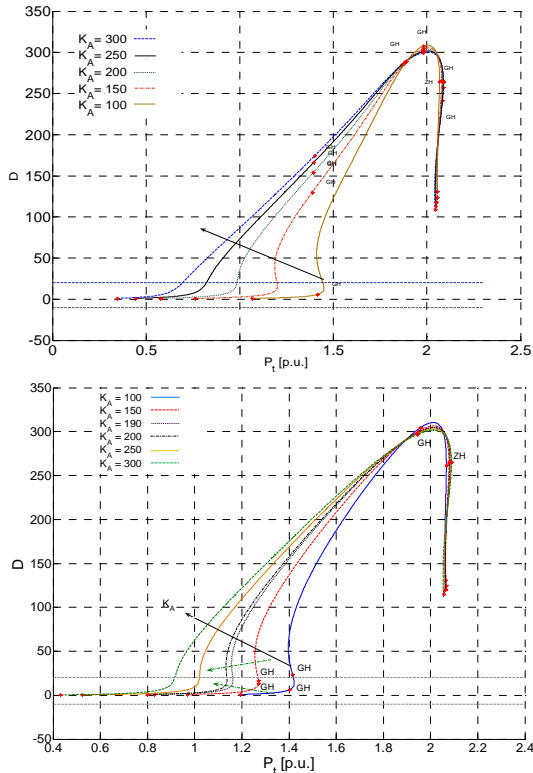


Figure 4. Effect of K_A on the Hopf bifurcation curve a) with the limiter; b) without the limiter

In Figure 5b an increase of V_{ref} causes an increase of the value of P_t at which the first PD occurs; the effect of this parameter is significant, as for a small V_{ref} variation equal to 0.05 p.u. a significant P_t variation (equal to about 0.1 p.u.) occurs. Moreover an increase of K_A causes the first PD curve to move towards lower values of P_t , besides causing a decrease of the value of V_{ref} at which the GPD occurs.

Figure 6 shows the first PD curves in the plane $P_t - D$ when V_{ref} and K_A vary. In Figure 6a one can notice that the increase of the AVR gain K_A causes the first PD curve to move towards lower values of P_t . On the contrary the change in K_A has little effect on the maximum value of the first PD curve, which is always detected around $P_t=1.55$ p.u.

In Figure 6b an increase of V_{ref} causes the first PD curve to move to higher values of P_t and the abscissa of the maximum moves to higher values of P_t . Moreover the change of V_{ref} has effects on the shape of the curve; in fact if V_{ref} diminishes the curve becomes wider.

D and V_{ref} being equal (to 2 and 1.05 p.u. respectively), Table 2 indicates the value of P_t at which the first (PD2), the second (PD4) and the third (PD8) PDs occur for different values of K_A .

Table 2. P_t versus PDS for some values of K_A

	K_A [p.u./p.u.]				
	100	150	190	250	300
PD2	1.306	1.151	1.047	0.923	0.841
PD4	1.327	1.310	1.300	1.291	1.286
PD8	1.332	1.316	1.309	1.302	1.298

a) The effect of K_A on the values of P_t diminishes if one passes from the first PD to the second PD and so on.

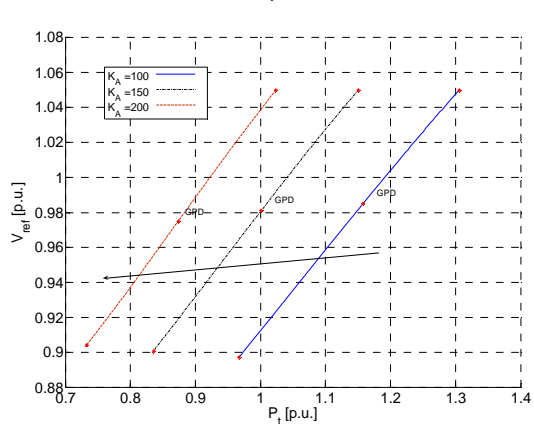
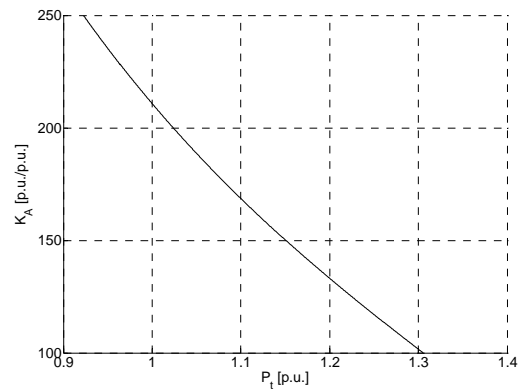


Figure 5. a) Effect of K_A on the first PD curve ($V_{ref}=1.05$ and $D=2$); b) Effect of V_{ref} on the first PD curve ($D=2$ and $K_A=100/150/200$)

PD bifurcations are strictly related to the chaos type investigated.

In the present paper the measure of chaos is carried out through the Lyapunov exponents (LE) which are calculated by running a proper function called *Lyapunov* and developed in [10]. This function does not belong to the adopted toolbox, MATCONT, and it implements the LE calculation algorithm described in [11].

Being D equal to 2, Table 3 indicates the value of P_t at which chaos starts for different values of V_{ref} and K_A .

Table 3. Values of P_t (in p.u.) at which chaos starts for some pairs of values of K_A and V_{ref}

K_A [p.u./p.u.] \ V_{ref} [p.u.]	1.00	1.02	1.05
300	1.193	1.235	1.300
250	1.195	1.238	1.304
225	1.196	1.240	1.306
200	1.198	1.242	1.309

Figure 7 visualizes the data of Table 3; it clearly shows that if the voltage setpoint diminishes, as well as if the gain K_A increases, chaos starts for lower values of P_t . The major effect on the value of P_t is due to V_{ref} .

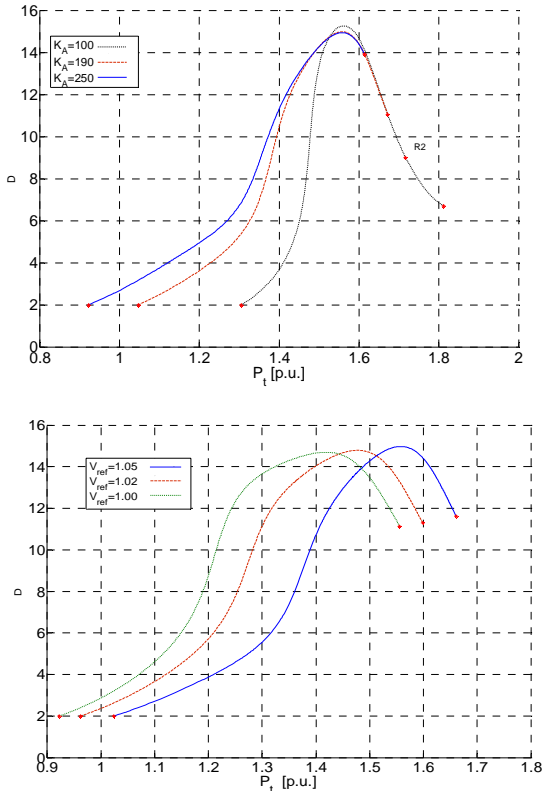


Figure 6. First PD curves a) when K_A varies (with $V_{ref} = 1.05$ p.u.); b) when V_{ref} varies (with $K_A = 200$ p.u./p.u.)

IV. FURTHER REMARKS AND CONCLUSIONS

The paper presents some results of the application of the NCM (Numerical Continuation Method) to a simple power system. The paper focuses above all on the system configuration with the voltage limiter. The first results reveal the complex behaviour of the simple power system for a precise interval of P_t , where there are two stable invariants (period-1 and period-2 cycles) separated by an unstable cycle. The study of the Hopf bifurcation curve allows to state that the presence of the limiter causes the generation of stable cycles on the right of this curve, which are not present if the limiter is not activated. These stable cycles undergo subsequent period doublings leading to the Feigenbaum chaos, which is not observed if there is no limiter.

The continuation of the Hopf bifurcation curves in the plane $P_t - D$ highlights that the increase of the gain K_A causes the Hopf curve to move towards lower values of P_t ; thus, even if an increase of K_A is useful to diminish the steady state error of the regulator, a too large increase of K_A causes the birth of generator angle oscillations for mechanical powers close to the nominal value. On the contrary, the effect of an increase of V_{ref} is the movement of the Hopf curve towards higher P_t values in the same bifurcation plane, which makes oscillatory behaviours less probable for realistic P_t values.

As for the fold bifurcation curve, one can observe that the increase of K_A causes a slight increase of the value of P_t at which the system collapses; an increase of V_{ref} within a limited range causes a significant increase of the value of P_t .

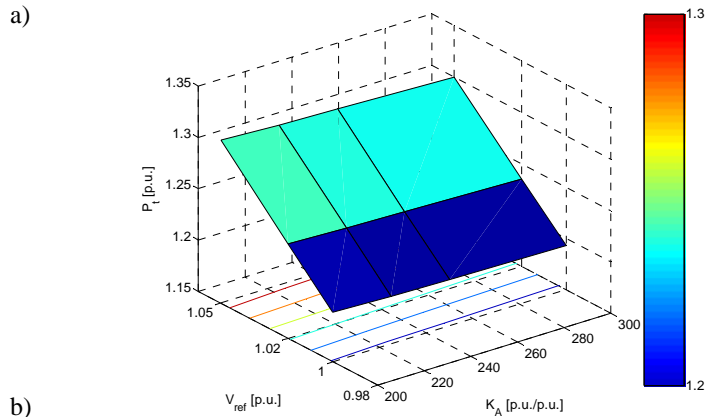


Figure 7. Chaos trigger surface in the parameter space $K_A - P_t - V_{ref}$

At last, the effect of the two aforementioned parameters on the PD curves has been analyzed; an increase of K_A causes these curves to move to lower and lower values of P_t , while it has a negligible effect on the maximum value of the curve (at least for the first PD); the effect of the gain K_A is less and less important when one passes from the first PD to the second PD and so on. With reference to Figure 6, it can be noticed that a decrease of V_{ref} (ranging from 1.00 p.u. to 1.05 p.u. in Figure 6) causes the first PD curve to move towards lower values of P_t and it is also responsible for an enlargement of the same curve.

As for chaos, a decrease of V_{ref} as well as an increase of K_A lowers the value of P_t at which chaos starts.

At last, damping factor D being equal to a realistic value, 2, the effect of K_A on the value of P_t which triggers chaos is significantly weaker than the effect of V_{ref} .

V. REFERENCES

- [1] F. Saccomanno, *Electric Power Systems: Analysis and Control*, IEEE Press Series on Power Engineering, 2003, pp. 30-32, ISBN: 0-471-23439-7
- [2] P. Kundur, *Power System Stability and Control*, 1994, EPRI Power System Engineering Series, pp. 35-36, ISBN: 9780070359581
- [3] V. Ajjarapu and B. Lee, "Bifurcation theory and its application in nonlinear dynamical phenomena in an electrical power system", *IEEE Transactions on Power Systems*, vol.17, No.1, pp. 424-131, Febr 1992
- [4] C.W. Tan, M. Verghese, P. Varaiya, F.F. Wu, "Bifurcation, Chaos and Voltage Collapse in Power Systems", *Proceedings of the IEEE Special issue on Nonlinear phenomena in Power Systems*, Vol. 83, No.11, pp. 1484-1539, November 1995
- [5] A. A. P. Lerm, C. A. Canizares, F. A. B. Lemos, A. S. e Silva, "Multi-parameter Bifurcation Analysis of Power Systems", *North American Power Symposium (NAPS)*, Oct 1998, Cleveland, Ohio
- [6] Z. Jing, D. Xu, Y. Chang, L. Chen, "Bifurcations, chaos, and system collapse in a three node power system", *Electrical Power & Energy Systems*, 2003, Elsevier
- [7] Yu. A. Kuznetsov, *Elements of Applied Bifurcation Theory*, 3rd ed., New York, Springer-Verlag, 2004
- [8] S. H. Strogatz, *Nonlinear Dynamics and Chaos*, Reading - MA, Addison-Wesley, 1994
- [9] W. Govaerts, Yu. A. Kuznetsov, A. Dhooge, "MATCONT: A MATLAB Package for Numerical Bifurcation Analysis of ODEs", *ACM Transactions on Mathematical Software*, Vol. 29, No. 2, pp. 141-164, June 2003
- [10] Govorukhin's website at www.math.rsu.ru
- [11] A. Wolf, J. B. Swift, H. L. Swinney, J. A. Vastano, "Determining Lyapunov Exponents from a Time Series", *Physica D*, Vol. 16, pp. 285-317, 1985

VI. BIOGRAPHIES

Samuele Grillo was born in Alessandria, Italy, in 1980. He received the "Laurea" degree in electronic engineering in 2004 and the PhD degree in electrical engineering 2008, both from the University of Genoa. His research interests are optimization, automatic control, neural networks and machine learning and their application to power systems.

Stefano Massucco received the Doctor degree in electrical engineering at the University of Genoa, Italy, in 1979. From 1979 to 1987, he had been working at the Electrical Engineering Department of Genoa University, at CREL - the Electrical Research Center of ENEL (Italian Electricity Board) in Milano, Italy, and at ANSALDO S.P.A. in Genoa, Italy. He has been Associate Professor of Power Systems at the University of Pavia and since 1993 at the Electrical Engineering Department, University of Genoa, as Full Professor since 2000. His research interests are in power systems and distributed generation modelling, control, and management. He is a member of CIGRE Working Group 601 of Study Committee C4 for "Review of on-line Dynamic Security Assessment Tools and Techniques".

Andrea Morini was born in Milano in 1964. He obtained his Laurea Degree in Electrical Engineering in 1990 and his PhD in Electrical Engineering – Electric Power System in 1994. From 1994 to 1999 he had been with Gensym Corporation working on Artificial Intelligence applications to Industrial Processes. Since 1999 he has been Assistant Professor at the Electrical Engineering Dept. University of Genova. He is regional in charge of AIDI – Italian Association for Lighting. He is also scientific in charge of National Projects, and also a member of AEIT and IEEE – PES.

Andrea Pitto was born in Genoa on March 2, 1981. He received his Doctor degree in Electrical Engineering at the University of Genoa, Italy, in 2005. He also received a PhD in Electrical Engineering at the same university in 2009. He is currently a research assistant at the Electrical Engineering Department of the University of Genoa. His area of interest includes probabilistic and deterministic approaches to power system security assessment, DG modelling, control and interface with distribution networks, application of bifurcation theory techniques to power systems analysis.

Federico Silvestro received the degree in electrical engineering from the University of Genoa in 1998 and a Ph.D. in power systems in 2002, with a dissertation on artificial intelligence applications to power systems. He is now under contract as Research Assistant at the Electric Engineering Department, University of Genoa, where he is working in power system simulators, security assessment, knowledge based systems applied to power systems.